VIII International Conference on Computational Methods for Coupled Problems in Science and Engineering
COUPLED PROBLEMS 2019
E. Oñate, M. Papadrakakis and B. Schrefler (Eds)

GENERIC BASED THERMODYNAMICALLY CONSISTENT DISCRETISATION IN SPACE AND TIME FOR OPEN THERMOMECHANICAL SYSTEMS

Mark Schiebl and Peter Betsch*

*Institute of Mechanics, Karlsruhe Institute of Technology, Germany
Otto-Ammann-Platz 9, 76131 Karlsruhe
{mark.schiebl,peter.betsch}@kit.edu, www.ifm.kit.edu

Key words: Coupled Systems, Thermomechanics, Structure-preserving Integrators

Abstract. In the present contribution structure-preserving numerical methods for finite strain thermoelastodynamics are proposed. The underlying variational formulation is based on the GENERIC formalism and makes possible the free choice of the thermodynamic state variable. The notion 'GENERIC consistent space discretization' is introduced which facilitates the design of Energy-Momentum-Entropy (EME) consistent schemes. In particular, three alternative EME schemes result from the present approach. These schemes are directly linked to the respective choice of the thermodynamic variable. A numerical example confirms the structure-preserving properties of the newly developed EME schemes, which exhibit superior numerical stability.

Since the pioneering work in [1], Energy-Momentum (EM) schemes established themselves in the field of nonlinear elastic solids and structures. Elastic solids and structures such as geometrically exact beams and shells fall into the framework of Hamiltonian systems with symmetry. EM schemes preserve main structural properties of the underlying reversible systems. In particular, by design, they correctly reproduce the balance laws for angular momentum and energy in the discrete setting. This way EM schemes often yield superior numerical stability and robustness. For more details on EM schemes, we refer the interested reader to [2, 3].
In the present work we aim at the extension of EM schemes to mechanical systems with dissipation. In particular, we focus on large-strain thermoelasticity. For that purpose, GENERIC (General Equation for Non-Equilibrium Reversible-Irreversible Coupling) provides an appealing framework since it recovers the Hamiltonian description in the absence of dissipative processes. In other words, GENERIC provides a natural extension of Hamiltonian mechanics to dissipative mechanical systems.
GENERIC was originally developed in the context of complex fluids (see [4] for a comprehensive account of the GENERIC framework) and later applied to solid mechanics, see [5, 6] and [7]. The GENERIC framework was first applied to computational solid mechanics in [8, 9] who coined the notion 'thermodynamically consistent (TC) integrator'. Alternatively, [10] recently introduced 'GENERIC integrators' which can be regarded as extension of symplectic integrators for Hamiltonian systems to the realm of dissipative systems.

Another advantageous feature of the GENERIC framework is that it facilitates the use of different sets of independent state variables (see [4] and [7]). The entropy was initially preferred as thermodynamic state variable in GENERIC-based integrators (see [8, 9] and [11, 12]). The work by [7] has laid the theoretical foundation for the development of GENERIC-based integrators relying on the temperature as thermodynamic state variable, see [13], [14] and [15]. In particular, in [7] a *special form of GENERIC* is devised which makes possible the free choice of the thermodynamic state variable. Mielke's procedure inspired further work on GENERIC-based integrators for finite-dimensional mechanical systems in [16] and finite-strain thermoelasticity in [17]. In particular, in [17] a GENERIC-based weak form is derived which makes possible the free choice of the thermodynamic state variable.
The GENERIC-based weak form in [17] provides the starting point for the development of Energy-Momentum-Entropy (EME) schemes (see [18] for more details). It was shown in [17] that the application of the standard mid-point rule already yields structure-preserving schemes. For example, choosing the internal energy density as thermodynamic state variable leads to an Energy-Momentum scheme. On the other hand, choosing the entropy density as thermodynamic state variable yields a Momentum-Entropy scheme. However, despite of their structure-preserving properties, all of the mid-point type schemes considered in [17] turned out to be prone to numerical instabilities. These observations led to the conjecture that only EME schemes will exhibit superior numerical stability for dissipative systems in the same way as do EM schemes for Hamiltonian systems.
Of course, the GENERIC framework is not a prerequisite for the development of structure-preserving numerical methods for non-isothermal solid mechanics. In the context of coupled thermomechanical problems alternative procedures have been proposed in [19], [20], [21] and [22].
As has been outlined above, the main goal of the present work is the development of EME schemes for large-strain thermoelasticity, starting from the GENERIC-based weak form developed in [17]. Correspondingly, Section 1 deals with large-strain thermoelasticity which includes the GENERIC-based weak form. In Section 2 the GENERIC-based weak form is discretized in space, resulting in a GENERIC-consistent space discretization. In Section 3, the semi-discrete system is further discretized in time leading to three alternative EME schemes. Section 4 contains a respresentative numerical example which confirms both the structure-preserving features and the enhanced numerical stability of the newly developed EME schemes when compared to the mid-point type schemes developed in [17]. Eventually, conclusions are drawn in Section 5.

1 Large-strain thermoelasticty

In this section we summarize the variational formulation of large-strain thermoelasticty with heat conduction which lies at the heart of the proposed discretization in space and time. This variational formulation has originally been developed in the context of the GENERIC framework (see [17] for more details).

1.1 Underlying variational formulation

We consider a continuum body with material points $\mathbf{X} = X_i \mathbf{e}_i$ in the reference configuration $\mathcal{B} \subset \mathbb{R}^3$, see Fig. 1. Here and in the sequel the summation convention applies to

repeated indices. Moreover, $\mathbf{e}_i$ denote the canonical base vectors in $\mathbb{R}^3$.

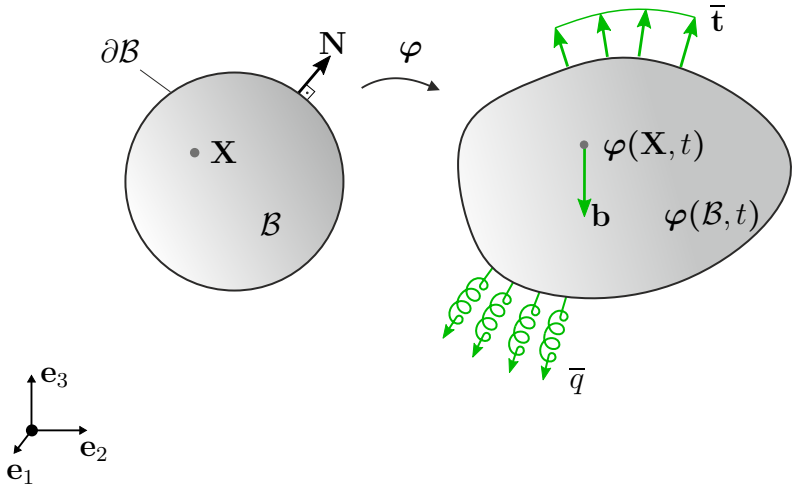

Figure 1: Reference configuration $\mathcal{B}$ with boundary $\partial\mathcal{B}$ and current configuration $\boldsymbol{\varphi}(\mathcal{B},t)$ at time t. External tractions $\overline{\mathbf{t}} = \mathbf{P}\mathbf{N}$ act on the boundary of the current configuration. In addition to that, the heat flux across the current boundary is denoted by $\overline{q} = \mathbf{Q}\cdot\mathbf{N}$. Here, the vector $\mathbf{N}$ denotes the unit outward normal field on the boundary $\partial\mathcal{B}$ of the reference configuration.

Within the Lagrangian description of continuum mechanics the deformed configuration of the body at time t is characterised by the deformation map $\boldsymbol{\varphi} : \mathcal{B}\times\mathcal{I} \mapsto \mathbb{R}^3$, where $\mathcal{I} = [0,T]$ is the time interal of interest. The velocity of the material point $\mathbf{X} \in \mathcal{B}$ located at $\mathbf{x} = \boldsymbol{\varphi}(\mathbf{X},t)$ is given by $\mathbf{v} = \dot{\boldsymbol{\varphi}}$, where a superposed dotes denotes the material time derivate. The deformation gradient is given by $\mathbf{F} = \partial\boldsymbol{\varphi}/\partial\mathbf{X}$. In what follows the partial derivative with respect to the material coordinates will often be denoted by the nabla operator. Accordingly, the deformation gradient assumes the form

$$\mathbf{F} = \nabla\boldsymbol{\varphi} \tag{1}$$

Main ingredients of the GENERIC framework are the internal energy and the entropy. In addition to that, the choice of the thermodynamic variable plays an important role. Similar to [7], we allow for the free choice of the thermodynamic variable $\tau : \mathcal{B}\times\mathcal{I} \mapsto \mathbb{R}$ from among three options $\tau \in \{\theta,\eta,u\}$. These options are (i) the absolute temperature θ, (ii) the entropy density η, and (iii) the internal energy density u. Depending on the choice of the thermodynamic variable, the absolute temperature can be written in the form (see also [4] and [7])

$$\theta = \theta'(\mathbf{C},\tau) = \frac{\partial_\tau u'(\mathbf{C},\tau)}{\partial_\tau \eta'(\mathbf{C},\tau)} \tag{2}$$

Here, the internal energy density and the entropy density, respectively, are given by

$$u = u'(\mathbf{C},\tau), \quad \eta = \eta'(\mathbf{C},\tau) \tag{3}$$

In this connection, a frame-indifferent constitutive formulation for thermoelastic materials is based on the right Cauchy-Green tensor $\mathbf{C} = \mathbf{F}^{\mathrm{T}}\mathbf{F}$. The GENERIC-based weak form

pertaining to large-strain thermoelasticity can be written in the form (see [17])

$$
\begin{aligned}
0 &= \int_{\mathcal{B}} \mathbf{w}_{\varphi} \cdot \left(\dot{\boldsymbol{\varphi}} - \rho^{-1} \mathbf{p} \right) \mathrm{d}V \\
0 &= \int_{\mathcal{B}} \left(\mathbf{w}_{\mathrm{p}} \cdot (\dot{\mathbf{p}} - \mathbf{b}) + \mathbf{F}\mathbf{S} : \nabla \mathbf{w}_{\mathrm{p}} \right) \mathrm{d}V - \int_{\partial_{\sigma}\mathcal{B}} \mathbf{w}_{\mathrm{p}} \cdot \overline{\mathbf{t}} \, \mathrm{d}A \\
0 &= \int_{\mathcal{B}} \left(\mathrm{w}_{\tau} \dot{\tau} + \nabla(\rho^{-1}\mathbf{p}) : \left(\frac{\mathrm{w}_{\tau}}{\partial_{\tau}\eta'} 2\mathbf{F}\partial_{\mathbf{C}}\eta' \right) - \nabla \left(\frac{\mathrm{w}_{\tau}}{\partial_{\tau}u'} \right) \cdot \mathbf{Q} \right) \mathrm{d}V + \int_{\partial_q \mathcal{B}} \frac{\mathrm{w}_{\tau}}{\partial_{\tau}u'} \overline{q} \, \mathrm{d}A
\end{aligned}
\tag{4}
$$

where $\rho : \mathcal{B} \mapsto \mathbb{R}_+$ is the mass density in the reference configuration. Moreover, $\mathbf{p} : \mathcal{B} \times \mathcal{I} \mapsto \mathbb{R}^3$ is the linear momentum density and $\mathbf{b} : \mathcal{B} \mapsto \mathbb{R}^3$ represent prescribed body forces which, for simplicity, are assumed to be dead loads. The second Piola-Kirchhoff stress tensor is given by

$$
\mathbf{S} = \mathbf{S}'(\mathbf{C}, \tau) = 2 \left(\partial_{\mathbf{C}} u' - \frac{\partial_{\tau} u'}{\partial_{\tau} \eta'} \partial_{\mathbf{C}} \eta' \right) \tag{5}
$$

Furthermore, the material heat flux vector assumes the form

$$
\mathbf{Q} = \mathbf{Q}'(\mathbf{C}, \tau) = (\theta')^2 \mathbf{K}' \nabla \left(\frac{\partial_{\tau} \eta'}{\partial_{\tau} u'} \right) \tag{6}
$$

where $\mathbf{K} = \mathbf{K}'(\mathbf{C}, \tau)$ is the positive semi-definite material conductivity tensor. The weak form needs be supplemented with initial and boundary conditions, respectively. For that purpose, the boundary $\partial\mathcal{B}$ of the continuum body is decomposed into a displacement boundary $\partial_{\varphi}\mathcal{B}$, on which $\boldsymbol{\varphi} = \overline{\boldsymbol{\varphi}}$ is prescribed, and a traction boundary $\partial_{\sigma}\mathcal{B}$, on which the external traction $\overline{\mathbf{t}}$ is prescribed such that $\mathbf{P}\mathbf{N} = \overline{\mathbf{t}}$ (Fig. 2). In this connection, the standard relations $\partial_{\varphi}\mathcal{B} \cup \partial_{\sigma}\mathcal{B} = \partial\mathcal{B}$ and $\partial_{\varphi}\mathcal{B} \cap \partial_{\sigma}\mathcal{B} = \varnothing$ hold. Similarly, for the thermal part we consider the subsets $\partial_{\tau}\mathcal{B}$ and $\partial_q\mathcal{B}$, with the properties $\partial_{\tau}\mathcal{B} \cup \partial_q\mathcal{B} = \partial\mathcal{B}$ and $\partial_{\tau}\mathcal{B} \cap \partial_q\mathcal{B} = \varnothing$ (Fig. 3). The thermodynamic variable is prescribed on $\partial_{\tau}\mathcal{B}$, i.e. $\tau = \overline{\tau}$, whereas the heat flux is prescribed on $\partial_q\mathcal{B}$, i.e. $\mathbf{Q} \cdot \mathbf{N} = \overline{q}$.

The unknown fields are subject to initial conditions of the form $\boldsymbol{\varphi}(\cdot, 0) = \mathbf{X}$, $\mathbf{p}(\cdot, 0) = \rho \mathbf{v}_0$, and $\tau(\cdot, 0) = \tau_0$ in $\mathcal{B}$. Here, $\mathbf{v}_0$ is a prescribed velocity field and τ_0 is a prescribed field of the thermodynamic variable $\tau \in \{\theta, \eta, u\}$.

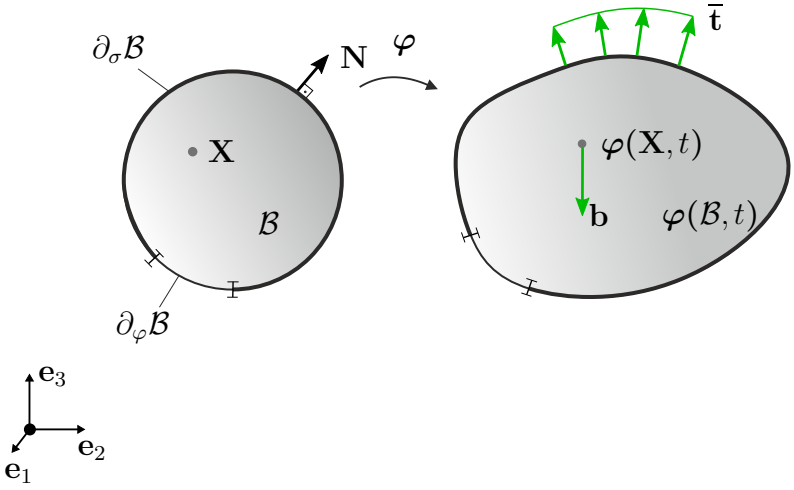

Figure 2: Mechanical part of the IBVP. Note that $\overline{\mathbf{t}} = \mathbf{P}\mathbf{N}$ denotes prescribed external Piola tractions acting on the current boundary expressed per unit area of the reference boundary $\partial_{\sigma}\mathcal{B}$.

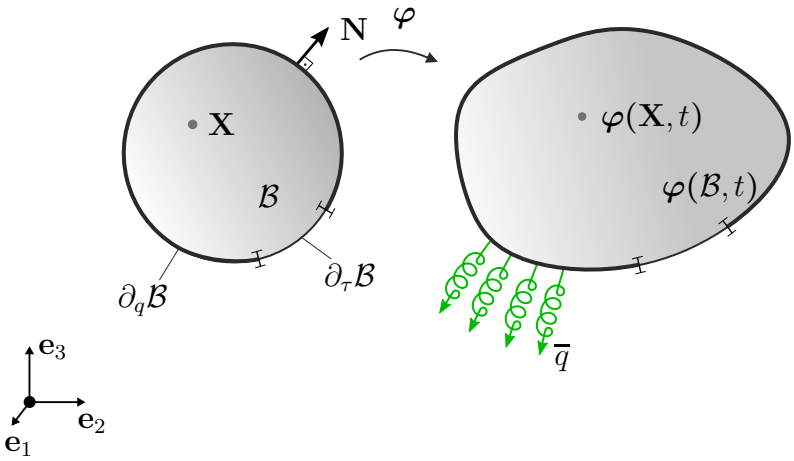

Figure 3: Thermal part of the IBVP. Note that $\overline{q} = \mathbf{Q} \cdot \mathbf{N}$ is the prescribed rate of heat transfer across the current boundary expressed per unit area of the reference boundary $\partial_q \mathcal{B}$.

2 Discretization in space

We next perform the discretization in space of the GENERIC-based weak form (4). To this end we apply the isoparametric finite element approach (see, for example, [23]), based on finite-dimensional approximations of the following quantities

$$\boldsymbol{\varphi}^{\mathrm{h}}(\mathbf{X}, t) = N^a(\mathbf{X})\, \mathbf{q}_a(t)\,, \qquad \mathbf{v}^{\mathrm{h}}(\mathbf{X}, t) = N^a(\mathbf{X})\, \mathbf{v}_a(t) \tag{7}$$

and

$$\tau^{\mathrm{h}}(\mathbf{X}, t) = N^a(\mathbf{X})\, \tau_a(t) \tag{8}$$

Here, the summation convention applies, where $a = 1, \dots, \mathrm{N}$, and N denotes the total number of nodes in the finite element mesh. Moreover, $N^a : \mathcal{B} \to \mathbb{R}$ are the nodal shape functions and $\mathbf{q}_a(t), \mathbf{v}_a(t) \in \mathbb{R}^3$, $\tau_a(t) \in \mathbb{R}$ are the respective nodal values at time t. Analogous approximations are used for the test functions $\mathbf{w}_\varphi, \mathbf{w}_{\mathrm{p}}$ and w_τ, denoted by $\mathbf{w}^{\mathrm{h}}_\varphi, \mathbf{w}^{\mathrm{h}}_{\mathrm{p}}$ and w^{h}_τ. Then weak form (4) leads to the following semi-discrete equations:

$$\begin{aligned}
0 &= \int_{\mathcal{B}} \mathbf{w}^{\mathrm{h}}_\varphi \cdot \left(\dot{\boldsymbol{\varphi}}^{\mathrm{h}} - \mathbf{v}^{\mathrm{h}} \right) \mathrm{d}V \\
0 &= \int_{\mathcal{B}} \left(\mathbf{w}^{\mathrm{h}}_{\mathrm{p}} \cdot \left(\rho \dot{\mathbf{v}}^{\mathrm{h}} - \mathbf{b} \right) + \nabla \mathbf{w}^{\mathrm{h}}_{\mathrm{p}} : \mathbf{F}^{\mathrm{h}} \mathbf{S}^{\mathrm{h}} \right) \mathrm{d}V - \int_{\partial_\sigma \mathcal{B}} \mathbf{w}^{\mathrm{h}}_{\mathrm{p}} \cdot \overline{\mathbf{t}}\, \mathrm{d}A \\
0 &= \int_{\mathcal{B}} \mathrm{w}^{\mathrm{h}}_\tau \left(\dot{\tau}^{\mathrm{h}} + \nabla \mathbf{v}^{\mathrm{h}} : \left(\frac{2}{\Pi_h(\partial_\tau \eta^{\mathrm{h}})} \mathbf{F}^{\mathrm{h}} \partial_{\mathbf{C}} \eta^{\mathrm{h}} \right) \right) \mathrm{d}V \\
&\quad - \int_{\mathcal{B}} \nabla \left(\frac{\mathrm{w}^{\mathrm{h}}_\tau}{\Pi_h(\partial_\tau u^{\mathrm{h}})} \right) \cdot \mathbf{Q}^{\mathrm{h}}\, \mathrm{d}V + \int_{\partial_q \mathcal{B}} \frac{\mathrm{w}^{\mathrm{h}}_\tau}{\Pi_h(\partial_\tau u^{\mathrm{h}})} \overline{q}\, \mathrm{d}A
\end{aligned} \tag{9}$$

where

$$\begin{aligned}
\mathbf{S}^{\mathrm{h}} &= 2 \left(\partial_{\mathbf{C}} u^{\mathrm{h}} - \Theta^{\mathrm{h}} \partial_{\mathbf{C}} \eta^{\mathrm{h}} \right) \\
\mathbf{Q}^{\mathrm{h}} &= (\Theta^{\mathrm{h}})^2 \mathbf{K}^{\mathrm{h}} \nabla \left(\frac{1}{\Theta^{\mathrm{h}}} \right) \\
\Theta^{\mathrm{h}} &= \frac{\Pi_h(\partial_\tau u^{\mathrm{h}})}{\Pi_h(\partial_\tau \eta^h)}
\end{aligned} \tag{10}$$

In this connection, $u^{\mathrm{h}} = u'(\mathbf{C}^{\mathrm{h}}, \tau^{\mathrm{h}})$, $\eta^{\mathrm{h}} = \eta'(\mathbf{C}^{\mathrm{h}}, \tau^{\mathrm{h}})$, and $\mathbf{K}^{\mathrm{h}} = \mathbf{K}'(\mathbf{C}^{\mathrm{h}}, \tau^{\mathrm{h}})$. The interpolation formulas in (7) give rise to

$$\mathbf{F}^{\mathrm{h}} = \mathbf{q}_a \otimes \nabla N^a \quad \text{and} \quad \mathbf{C}^{\mathrm{h}} = \mathbf{q}_a \cdot \mathbf{q}_b \nabla N^a \otimes \nabla N^b \tag{11}$$

Moreover, $\Pi_h(\partial_\tau u^{\mathrm{h}})$ denotes the L_2 projection of function $\partial_\tau u^{\mathrm{h}}$ into the finite-dimensional space spanned by the shape functions N^a, $a = 1, \dots, \mathrm{N}$. That is,

$$\Pi_h(\partial_\tau u^{\mathrm{h}}) = N^a (\partial_\tau u)_a \tag{12}$$

where the nodal values $(\partial_\tau u)_a$ are determined by

$$\int_{\mathcal{B}} N^a \left(\partial_\tau u^{\mathrm{h}} - \Pi_h(\partial_\tau u^{\mathrm{h}}) \right) \mathrm{d}V = 0 \tag{13}$$

for $a = 1, \dots, \mathrm{N}$. In particular, (13) together with (12) constitute a linear system of algebraic equations given by

$$H^{ab} (\partial_\tau u)_b = \int_{\mathcal{B}} N^a \partial_\tau u^{\mathrm{h}} \, \mathrm{d}V \tag{14}$$

where H^{ab} denote the components of the positive definite Gram matrix $[H^{ab}]$ defined by

$$H^{ab} = \int_{\mathcal{B}} N^a N^b \, \mathrm{d}V \tag{15}$$

Analogous relationships hold for the projection of function $\partial_\tau \eta^{\mathrm{h}}$, $\Pi_h(\partial_\tau \eta^{\mathrm{h}})$. It is worth mentioning that the projections $\Pi_h(\partial_\tau u^{\mathrm{h}})$ and $\Pi_h(\partial_\tau \eta^{\mathrm{h}})$ are only required if the functions $\partial_\tau u^{\mathrm{h}}$ and $\partial_\tau \eta^{\mathrm{h}}$ do not belong to the finite element space spanned by the shape functions N^a. For example, in the temperature-based formulation (i.e. for $\tau = \theta$), $\partial_\theta u^{\mathrm{h}} = \partial_\theta \overline{u}(\mathbf{C}^{\mathrm{h}}, \theta^{\mathrm{h}})$ corresponds to the specific heat at constant deformation. Thus, if this quantity is prescribed to be constant, the projection $\Pi_h(\partial_\theta \overline{u})$ need not be performed. However, in general the temperature-based formulation requires both projections (i.e. $\Pi_h(\partial_\theta \overline{u})$ and $\Pi_h(\partial_\theta \overline{\eta})$).
In contrast to that, the two alternative formulations based on the choice $\tau \in \{\eta, u\}$ in general require only one projection. In particular, the formulation in terms of the internal energy density relies on $\Pi_h(\partial_u \widetilde{\eta})$, whereas the entropy-based formulation relies on $\Pi_h(\partial_\eta \widetilde{u})$. Originally, the projection has been introduced in the framework of the entropy-based formulation in [9] (see also [12]).
The introduction of the above projections is essential for retaining consistency of the semi-discrete formulation and is therefore termed *GENERIC-consistent space discretization*, see [18] for more details.

3 Discretization in time

We aim at a second-order accurate, implicit time-stepping scheme which is capable of correctly reproducing the main balance laws outlined above. Due to its structure-preserving properties this type of integrator is called Energy-Momentum-Entropy (EME) scheme. To devise such a scheme, we essentially apply the mid-point rule in which the derivatives of the internal energy density and the entropy density, respectively, are replaced by appropriate discrete derivatives.

We focus on a representative time interval $[t_{\mathrm{n}}, t_{\mathrm{n+1}}]$ with corresponding time-step size $\Delta t = t_{\mathrm{n+1}} - t_{\mathrm{n}}$. The discrete approximations at times t_{n} and $t_{\mathrm{n+1}}$ of a function $f(t)$ will be denoted by f_{n} and $f_{\mathrm{n+1}}$, respectively. Assume that the nodal state variables at time t_{n}, $\mathbf{q}_{a_{\mathrm{n}}}$, $\mathbf{v}_{a_{\mathrm{n}}}$, and $\tau_{a_{\mathrm{n}}}$ are given. The associated fields result from the nodal interpolation formulas (7) and are denoted by $\boldsymbol{\varphi}^{\mathrm{h}}_{\mathrm{n}}, \mathbf{v}^{\mathrm{h}}_{\mathrm{n}} : \mathcal{B} \mapsto \mathbb{R}^3$ and $\tau^{\mathrm{h}}_{\mathrm{n}} : \mathcal{B} \mapsto \mathbb{R}$, $\tau \in \{\theta, \eta, u\}$. We aim at the determination of the corresponding quantities at time $t_{\mathrm{n+1}}$ through the mid-point type discretization of the semi-discrete formulation (9) given by

$$
\begin{aligned}
0 &= \int_{\mathcal{B}} \mathbf{w}^{\mathrm{h}}_{\varphi} \cdot \left(\frac{\boldsymbol{\varphi}^{\mathrm{h}}_{\mathrm{n+1}} - \boldsymbol{\varphi}^{\mathrm{h}}_{\mathrm{n}}}{\Delta t} - \mathbf{v}^{\mathrm{h}}_{\mathrm{n+\frac{1}{2}}} \right) \mathrm{d}V \\
0 &= \int_{\mathcal{B}} \left(\mathbf{w}^{\mathrm{h}}_{\mathrm{p}} \cdot \left(\rho \frac{\mathbf{v}^{\mathrm{h}}_{\mathrm{n+1}} - \mathbf{v}^{\mathrm{h}}_{\mathrm{n}}}{\Delta t} - \mathbf{b} \right) + \nabla \mathbf{w}^{\mathrm{h}}_{\mathrm{p}} : \mathbf{F}^{\mathrm{h}}_{\mathrm{n+\frac{1}{2}}} \mathbf{S}^{\mathrm{h}}_{\mathrm{alg}} \right) \mathrm{d}V - \int_{\partial_\sigma \mathcal{B}} \mathbf{w}^{\mathrm{h}}_{\mathrm{p}} \cdot \overline{\mathbf{t}} \, \mathrm{d}A \\
0 &= \int_{\mathcal{B}} \mathrm{w}^{\mathrm{h}}_{\tau} \left(\frac{\tau^{\mathrm{h}}_{\mathrm{n+1}} - \tau^{\mathrm{h}}_{\mathrm{n}}}{\Delta t} + \nabla \mathbf{v}^{\mathrm{h}}_{\mathrm{n+\frac{1}{2}}} : \left(\frac{2}{\Pi_h(\mathrm{D}_\tau \eta^{\mathrm{h}})} \mathbf{F}^{\mathrm{h}}_{\mathrm{n+\frac{1}{2}}} \mathrm{D}_{\mathbf{C}} \eta^{\mathrm{h}} \right) \right) \mathrm{d}V \\
&\quad - \int_{\mathcal{B}} \nabla \left(\frac{\mathrm{w}^{\mathrm{h}}_{\tau}}{\Pi_h(\mathrm{D}_\tau u^{\mathrm{h}})} \right) \cdot \mathbf{Q}^{\mathrm{h}}_{\mathrm{alg}} \, \mathrm{d}V + \int_{\partial_q \mathcal{B}} \frac{\mathrm{w}^{\mathrm{h}}_{\tau}}{\Pi_h(\mathrm{D}_\tau u^{\mathrm{h}})} \overline{q} \, \mathrm{d}A
\end{aligned}
\tag{16}
$$

where

$$
\begin{aligned}
\mathbf{S}^{\mathrm{h}}_{\mathrm{alg}} &= 2 \left(\mathrm{D}_{\mathbf{C}} u^{\mathrm{h}} - \Theta^{\mathrm{h}}_{\mathrm{alg}} \mathrm{D}_{\mathbf{C}} \eta^{\mathrm{h}} \right) \\
\mathbf{Q}^{\mathrm{h}}_{\mathrm{alg}} &= (\Theta^{\mathrm{h}}_{\mathrm{alg}})^2 \mathbf{K}'(\mathbf{C}^{\mathrm{h}}_{\mathrm{n+\frac{1}{2}}}, \tau^{\mathrm{h}}_{\mathrm{n+\frac{1}{2}}}) \nabla \left(\frac{1}{\Theta^{\mathrm{h}}_{\mathrm{alg}}} \right) \\
\Theta^{\mathrm{h}}_{\mathrm{alg}} &= \frac{\Pi_h(\mathrm{D}_\tau u^{\mathrm{h}})}{\Pi_h(\mathrm{D}_\tau \eta^h)}
\end{aligned}
\tag{17}
$$

The above discretization in time relies on the use of discrete derivatives in the sense of Gonzalez [24]. In particular, the discrete derivatives are applied to the internal energy density and the entropy density, respectively. For example, in the case of the internal energy density, the discrete derivatives are denoted by $\mathrm{D}_\tau u^{\mathrm{h}}$ and $\mathrm{D}_{\mathbf{C}} u^{\mathrm{h}}$, respectively. In particular, $\mathrm{D}_\tau u^{\mathrm{h}}$ is defined by

$$
\mathrm{D}_\tau u^{\mathrm{h}} = \frac{1}{2} \left(\mathrm{d}u_{\mathbf{C}^{\mathrm{h}}_{\mathrm{n}}}(\tau^{\mathrm{h}}_{\mathrm{n}}, \tau^{\mathrm{h}}_{\mathrm{n+1}}) + \mathrm{d}u_{\mathbf{C}^{\mathrm{h}}_{\mathrm{n+1}}}(\tau^{\mathrm{h}}_{\mathrm{n}}, \tau^{\mathrm{h}}_{\mathrm{n+1}}) \right)
\tag{18}
$$

where

$$
\mathrm{d}u_{\mathbf{C}}(\tau_{\mathrm{n}}, \tau_{\mathrm{n+1}}) = \partial_\tau u'(\mathbf{C}, \tau_{\mathrm{n+\frac{1}{2}}}) + \frac{u'(\mathbf{C}, \tau_{\mathrm{n+1}}) - u'(\mathbf{C}, \tau_{\mathrm{n}}) - \partial_\tau u'(\mathbf{C}, \tau_{\mathrm{n+\frac{1}{2}}}) \Delta\tau}{(\Delta\tau)^2} \Delta\tau
$$

and $\Delta\tau = \tau_{\mathrm{n+1}} - \tau_{\mathrm{n}}$. Furthermore, $\mathrm{D}_{\mathbf{C}} u^{\mathrm{h}}$ is defined by

$$
\mathrm{D}_{\mathbf{C}} u^{\mathrm{h}} = \frac{1}{2} \left(\mathrm{d}u_{\tau^{\mathrm{h}}_{\mathrm{n}}}(\mathbf{C}^{\mathrm{h}}_{\mathrm{n}}, \mathbf{C}^{\mathrm{h}}_{\mathrm{n+1}}) + \mathrm{d}u_{\tau^{\mathrm{h}}_{\mathrm{n+1}}}(\mathbf{C}^{\mathrm{h}}_{\mathrm{n}}, \mathbf{C}^{\mathrm{h}}_{\mathrm{n+1}}) \right)
\tag{19}
$$

where

$$
\mathrm{d}u_{\tau}(\mathbf{C}_{\mathrm{n}}, \mathbf{C}_{\mathrm{n+1}}) = \partial_{\mathbf{C}} u'(\mathbf{C}_{\mathrm{n+\frac{1}{2}}}, \tau) + \frac{u'(\mathbf{C}_{\mathrm{n+1}}, \tau) - u'(\mathbf{C}_{\mathrm{n}}, \tau) - \partial_{\mathbf{C}} u'(\mathbf{C}_{\mathrm{n+\frac{1}{2}}}, \tau) : \Delta\mathbf{C}}{\Delta\mathbf{C} : \Delta\mathbf{C}} \Delta\mathbf{C}
$$

and $\Delta\mathbf{C} = \mathbf{C}_{n+1} - \mathbf{C}_n$. It can be verified by a straightforward calculation that the discrete derivatives (18) and (19) satisfy the directionality condition

$$\mathrm{D}_{\mathbf{C}} u^h : \left(\mathbf{C}^h_{n+1} - \mathbf{C}^h_n\right) + \mathrm{D}_\tau u^h \left(\tau^h_{n+1} - \tau^h_n\right) = u'(\mathbf{C}^h_{n+1}, \tau^h_{n+1}) - u'(\mathbf{C}^h_n, \tau^h_n) \tag{20}$$

Analogous considerations apply to the discrete derivatives of the internal entropy density, $\mathrm{D}_\tau \eta^h$ and $\mathrm{D}_{\mathbf{C}} \eta^h$, respectively. Moreover, the time-average of any quantity $(\bullet)$ is given by $\frac{1}{2}\left((\bullet)_n + (\bullet)_{n+1}\right)$. In particular, this implies

$$\mathbf{C}_{n+\frac{1}{2}} = \frac{1}{2}\left(\mathbf{C}_n + \mathbf{C}_{n+1}\right) \tag{21}$$

Note that in general $\mathbf{C}_{n+\frac{1}{2}} \neq \mathbf{F}^T_{n+\frac{1}{2}} \mathbf{F}_{n+\frac{1}{2}}$.

4 Numerical example

The numerical example deals with a rotating disc subjected to a prescribed heat flow over one quarter of the lateral boundary surface (Fig. 4), where the material model can be found in [17, 18]. The disc is discretized using 200 tri-linear finite elements leading to a total of 360 nodes. The prescribed heat flow vector as well as the initial velocity distribution over the disc, which results from a prescribed constant angular velocity $\boldsymbol{\omega}_0 \in \mathbb{R}^3$, are given by

$$\mathbf{v}_0(\mathbf{X}) = \boldsymbol{\omega}_0 \times \mathbf{X}, \qquad \boldsymbol{\omega}_0 = \begin{pmatrix} 1 \\ 1 \\ 1 \end{pmatrix} \frac{1}{\mathrm{s}}, \qquad \overline{q} = -\frac{2000W}{\pi \mathrm{m}^2} f(t), \qquad f(t) = \begin{cases} \sin(2\frac{\pi}{4}t) & \text{for} \quad 0 \leq t \leq 4 \\ 0 & \text{for} \quad t > 4 \end{cases}$$

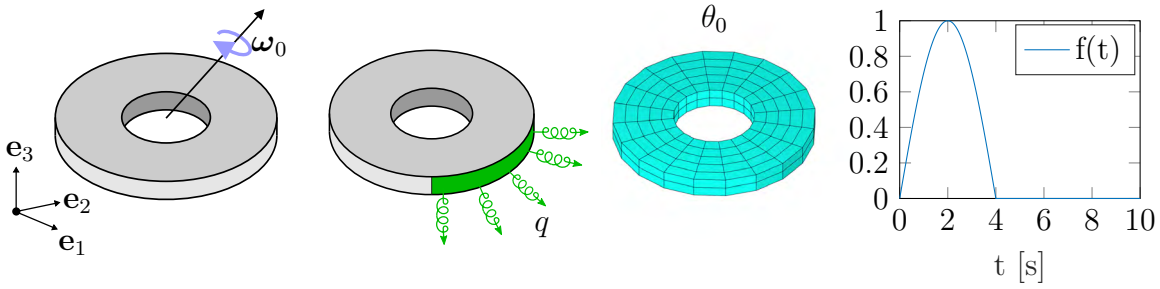

Figure 4: Rotating disc: Initial configuration (left), thermal boundary conditions (middle left), discrete disc (middle right), along with function $f(t)$ for the prescribed heat flow over part of the boundary surface (right)

The initial temperature of the disc is homogeneously distributed and equal to the reference temperature θ_0. The heat flow is prescribed over one quarter of the lateral boundary surface (Fig. 4) during an initial period of time, $t \in [0, 4]$s. In Fig. 4 a plot of function $f(t)$ can be found. The rest of the boundary of the disc is assumed to be thermally insulated ($\overline{q} = 0$). After $t = 4s$ the prescribed heat flow vanishes as well. A summary of the data used in the simulation of the rotating disc can be found in Table 1.

Table 1: Rotating disc: Data used in the simulations

Material parameters	λ	3000	Pa
	μ	750	Pa
Specific heat capacity	c	150	$\mathrm{JK^{-1}m^{-3}}$
Coupling coefficient	β	$1 \cdot 10^{-4}$	$\mathrm{JK^{-1}}$
Thermal conductivity	k	20	$\mathrm{WK^{-1}m^{-1}}$
Ref. temperature	θ_0	300	K
Mass density	ρ	8.93	$\mathrm{kgm^{-3}}$
Radius	r_i	0.8	m
	r_a	2	m
Thickness	t	0.4	m
Newton tolerance	ε	10^{-8}	-
Simulation time	T	30	s
Time step	Δt	0.1	s

Geometry of the rotating disc

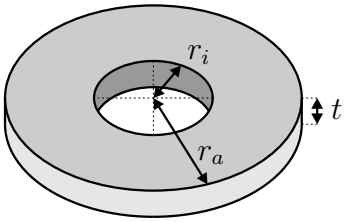

During initial period $t \in [0, 4]$s the total energy of the system is expected to increase due to the prescribed heat flow into the system. After initial period the system is classified as closed and therefore the total energy of the system should stay constant. All $(\mathrm{EME})_\tau$ integrators are capable to correctly reproduce the first law of thermodynamics (see Fig. 5) in contrast to the midpoint-based schemes, where only the formulation in the internal energy density was in accordance with the first law of thermodynamics, see [17].

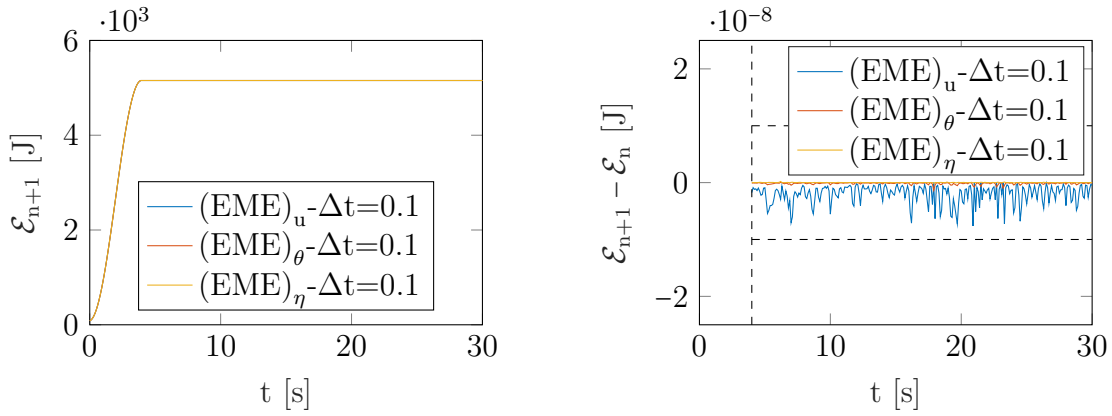

Figure 5: Rotating disc: Total energy (left) and incremental change of total energy (right)

The total entropy of the system is expected to increase due to the prescribed heat flow into the system during the initial period $t \in [0, 4]$s. As the system is closed after the initial period, the total entropy of the system should be a non-decreasing function, whereby the irreversibility is caused by heat conduction. All $(\mathrm{EME})_\tau$ integrators correctly reproduce the second law of thermodynamics as can be observed from Fig. 6. Again this is in contrast to the mid-point-based schemes investigated in [17], where only the formulation in terms of the entropy density was shown to be consistent with the second law.

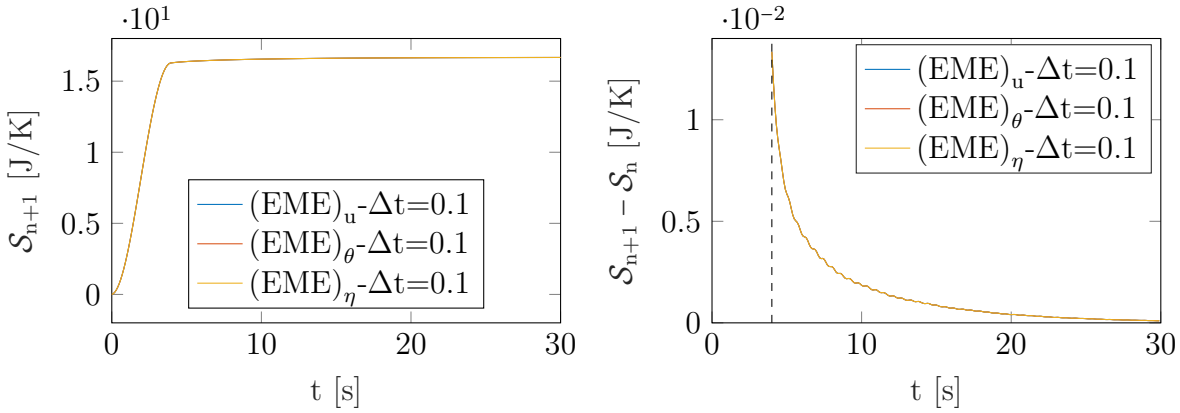

Figure 6: Rotating disc: Total entropy (left) and incremental change of total entropy (right)

Eventually, the motion of the disc is illustrated in Fig. 7 with snapshots at successive points in time. In addition to that, the distribution of the temperature over the disc is shown.

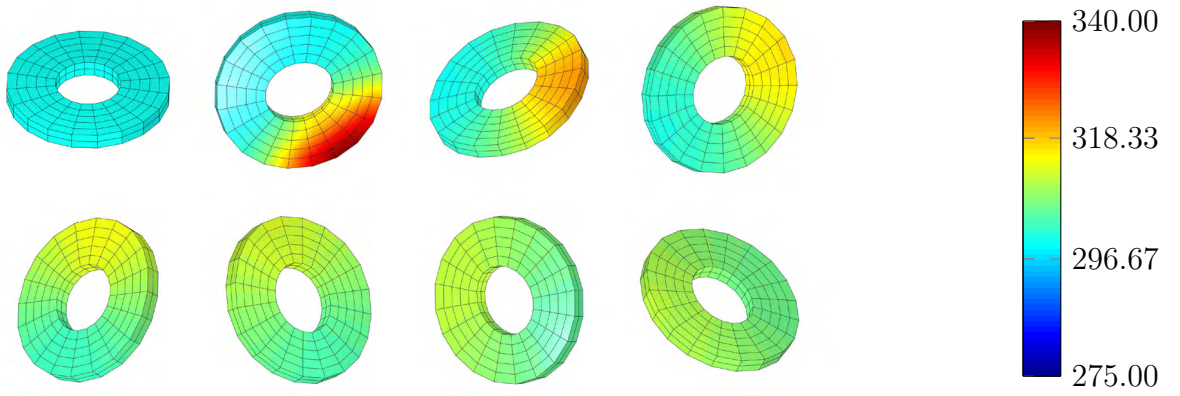

Figure 7: Rotating disc: Snapshots of the motion at successive points in time $t \in \{0, 4, 8, 12, 16, 18, 24, 28\}$s, and corresponding temperature distribution, calculated with the (EME)$_\theta$ scheme and Δt= 0.1s

5 Conclusions

Starting from the GENERIC-based weak form (4) we have newly developed structure-preserving numerical methods for finite strain thermoelasticity with heat conduction. The proposed Energy-Momentum-Entropy (EME) schemes make possible the free choice of the thermodynamic state variable. In particular, one may choose from among three options which include the entropy density, the absolute temperature and the internal energy density. Each choice of the thermodynamic variable ($\tau \in \{\eta, \theta, u\}$) leads to a corresponding (EME)$_\tau$ scheme.

The underlying GENERIC-based weak form has proven to be especially well-suited for the design of structure-preserving schemes. Depending on the choice of the thermodynamic variable τ, the application of the standard mid-point rule already leads to partially

structure-preserving schemes. For example, it was shown in [17] that the choice of the entropy density yields a Momentum-Entropy scheme, whereas the choice of the internal energy density yields an Energy-Momentum scheme. However, despite of their structure-preserving properties, all of the mid-point based schemes turned out to be prone to numerical instabilities (see [17]).
With regard to the discretization in space we have newly introduced the notion *GENERIC-consistent space discretization*. We have seen that the present discretization in space relying on standard Lagrangian shape functions necessitates the use of specific projections to reach a GENERIC-consistent space discretization.
It was shown that the present EME schemes lead to a significant improvement in the numerical stabilty when compared to mid-point type schemes. It would be of interest to extend the present approach to more involved coupled thermomechanical problems which also account for inelastic deformations.

References

[1] J.C. Simo and N. Tarnow. The discrete energy-momentum method. Conserving algorithms for nonlinear elastodynamics. *Z. angew. Math. Phys. (ZAMP)*, 43:757–792, 1992.

[2] P. Betsch, editor. *Structure-preserving Integrators in Nonlinear Structural Dynamics and Flexible Multibody Dynamics*, volume 565 of *CISM Courses and Lectures*. Springer-Verlag, 2016.

[3] P. Betsch. Computational dynamics. In H. Altenbach and A. Öchsner, editors, *Encyclopedia of Continuum Mechanics*, pages 1–11. Springer-Verlag, 2018.

[4] H.C. Öttinger. *Beyond Equilibrium Thermodynamics*. John Wiley & Sons, 2005.

[5] M. Hütter and B. Svendsen. On the formulation of continuum thermodynamic models for solids as general equations for non-equilibrium reversible-irreversible coupling. *J. Elast.*, 104(1-2):357–368, 2011.

[6] M. Hütter and B. Svendsen. Thermodynamic model formulation for viscoplastic solids as general equations for non-equilibrium reversible-irreversible coupling. *Continuum Mech. Thermodyn.*, 24(3):211–227, 2012.

[7] A. Mielke. Formulation of thermoelastic dissipative material behavior using GENERIC. *Continuum Mech. Thermodyn.*, 23(3):233–256, 2011.

[8] I. Romero. Thermodynamically consistent time-stepping algorithms for non-linear thermomechanical systems. *Int. J. Numer. Meth. Engng*, 79(6):706–732, 2009.

[9] I. Romero. Algorithms for coupled problems that preserve symmetries and the laws of thermodynamics: Part I: Monolithic integrators and their application to finite strain thermoelasticity. *Comput. Methods Appl. Mech. Engrg.*, 199(25-28):1841–1858, 2010.

[10] H.C. Öttinger. Generic integrators: Structure preserving time integration for thermodynamic systems. *Journal of Non-Equilibrium Thermodynamics*, 43(2):89–100, 2018.

[11] M. Krüger, M. Groß, and P. Betsch. A comparison of structure-preserving integrators for discrete thermoelastic systems. *Computational Mechanics*, 47(6):701–722, 2011.

[12] M. Krüger, M. Groß, and P. Betsch. An energy-entropy-consistent time stepping scheme for nonlinear thermo-viscoelastic continua. *ZAMM*, 96(2):141–178, 2016.

[13] S. Conde Martín, P. Betsch, and J.C. García Orden. A temperature-based thermodynamically consistent integration scheme for discrete thermo-elastodynamics. *Commun. Nonlinear Sci. Numer. Simulat.*, 32:63–80, 2016.

[14] S. Conde Martín. *Energy-Entropy-Momentum Time Integration Methods for Coupled Smooth Dissipative Problems*. PhD Dissertation, Universidad Politécnica de Madrid, 2016.

[15] S. Conde Martín and J.C. García Orden. On Energy-Entropy-Momentum integration methods for discrete thermo-visco-elastodynamics. *Computers & Structures*, 181:3–20, 2017.

[16] D. Portillo, J.C. García Orden, and I. Romero. Energy-entropy-momentum integration schemes for general discrete non-smooth dissipative problems in thermomechanics. *Int. J. Numer. Meth. Engng*, 112(7):776–802, 2017.

[17] P. Betsch and M. Schiebl. GENERIC-based formulation and discretization of initial boundary value problems for finite strain thermoelasticity. Submitted for publication, February 27 2019.

[18] P. Betsch and M. Schiebl. Energy-momentum-entropy consistent numerical methods for large strain thermoelasticity relying on the generic formalism. Submitted for publication, January 31 2019.

[19] M. Groß and P. Betsch. Galerkin-based energy-momentum consistent time-stepping algorithms for classical nonlinear thermo-elastodynamics. *Mathematics and Computers in Simulation*, 82(4):718–770, 2011.

[20] J.C. García Orden and I. Romero. Energy-Entropy-Momentum integration of discrete thermo-visco-elastic dynamics. *European Journal of Mechanics, A/Solids*, 32:76–87, 2012.

[21] M. Groß, M. Bartelt, and P. Betsch. Structure-preserving time integration of non-isothermal finite viscoelastic continua related to variational formulations of continuum dynamics. *Comput. Mech.*, 62(2):123–150, 2018.

[22] M. Franke, A. Janz, M. Schiebl, and P. Betsch. An energy-momentum consistent integration scheme using a polyconvexity-based framework for non-linear thermo-elastodynamics. *Int. J. Numer. Meth. Engng*, 155(5):549–577, 2018.

[23] T.J.R. Hughes. *The Finite Element Method*. Dover Publications, 2000.

[24] O. Gonzalez. Time integration and discrete Hamiltonian systems. *J. Nonlinear Sci.*, 6:449–467, 1996.